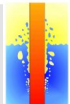
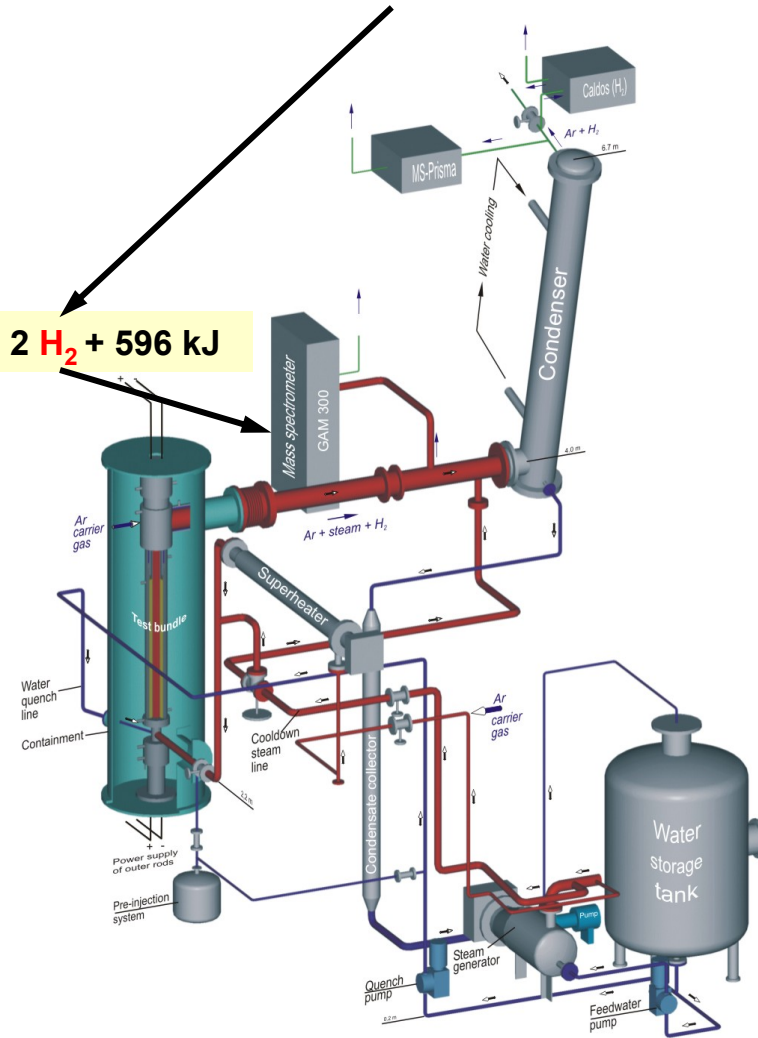
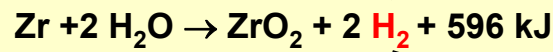
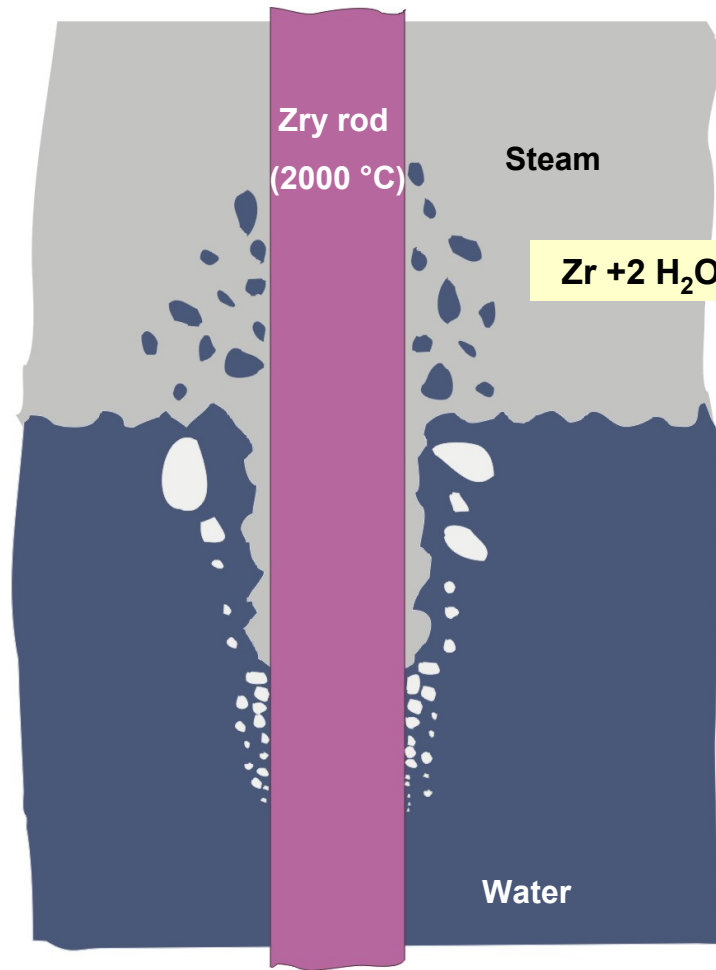


Experimental and Post-Test Calculation Results of the Integral Reflood Test QUENCH-12 with a VVER-type Bundle

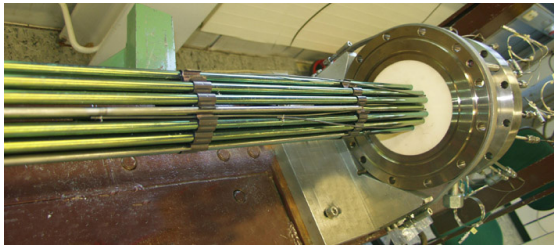
*J. Stuckert, M. Große, M. Steinbrück
Forschungszentrum Karlsruhe*



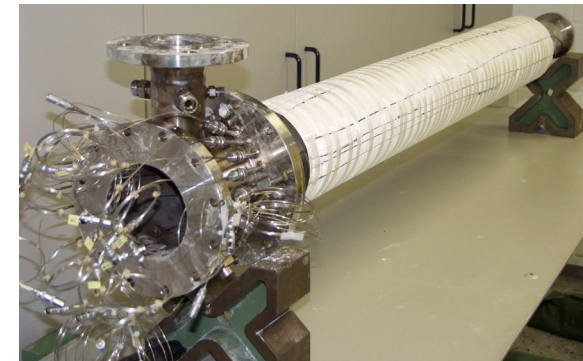
High-Temperature Materials Behavior and Flooding of an Overheated LWR Core and **Hydrogen Source Term**



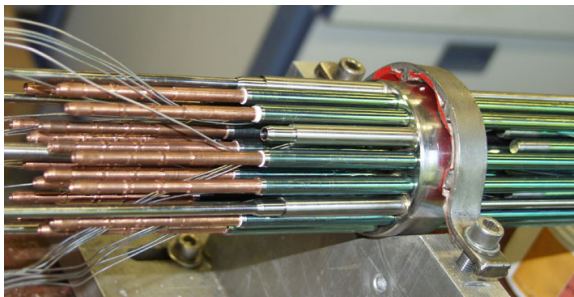
QUENCH-12 Test bundle assembling



bundle top



shroud with heat insulation



bundle bottom



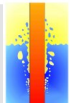
Test Matrix (1998-2008)

Test	Test date	Quench medium	Flooding rate, g/s	Remarks
QUENCH-01	Feb 26, 1998	Water	52	EC COBE
QUENCH-02	July 07, 1998	Water	47	EC COBE
QUENCH-03	Jan 20, 1999	Water	40	As Q-02 but flooding delayed
QUENCH-04	Juni 30, 1999	Steam	50	Steam, reference
QUENCH-05	March 29, 00	Steam	48	As Q-04 but with pre-oxidation
QUENCH-06	Dec 13, 2000	Water	42	OECD ISP-45; As Q-05 but with water flooding
QUENCH-07	July 25, 2001	Steam	15	EC COLOSS; B ₄ C absorber
QUENCH-08	July 24, 2003	Steam	15	As Q-07 but without B ₄ C absorber
QUENCH-09	July 03, 2002	Steam	49	EC COLOSS; As Q-07 but under steam starvation
QUENCH-10	July 21, 2004	Water	50	EC LACOMERA-1; Air ingress
QUENCH-11	Dec 8, 2005	Water	15	EC LACOMERA-2; Boil-off, SARNET-Benchmark
QUENCH-12	Sept 27, 2006	Water	48	ISTC 1648.2; VVER
QUENCH-13	Nov 7, 2007	Water	52	AgInCd absorber, SARNET-Aerosol
QUENCH-14	July 2, 2008	Water	41	ACM series: M5 [®] cladding

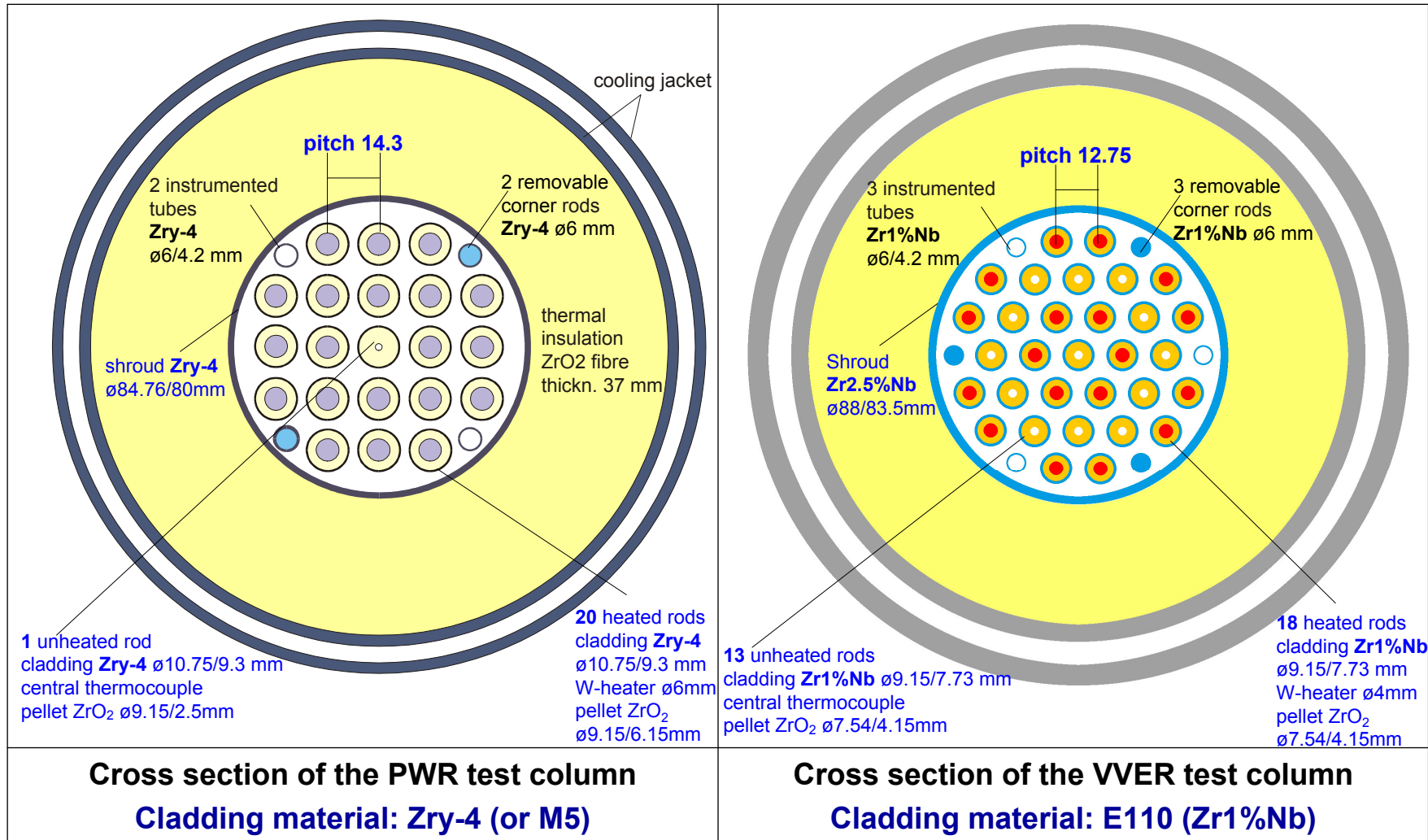


Objectives of the QUENCH-12 test

- **investigation of the effects of VVER materials and bundle geometry on core reflood**
- **comparison with the PWR bundle on the base of repeat of the test QUENCH-06 (ISP-45) scenario**



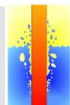
Comparison of PWR and VVER test columns



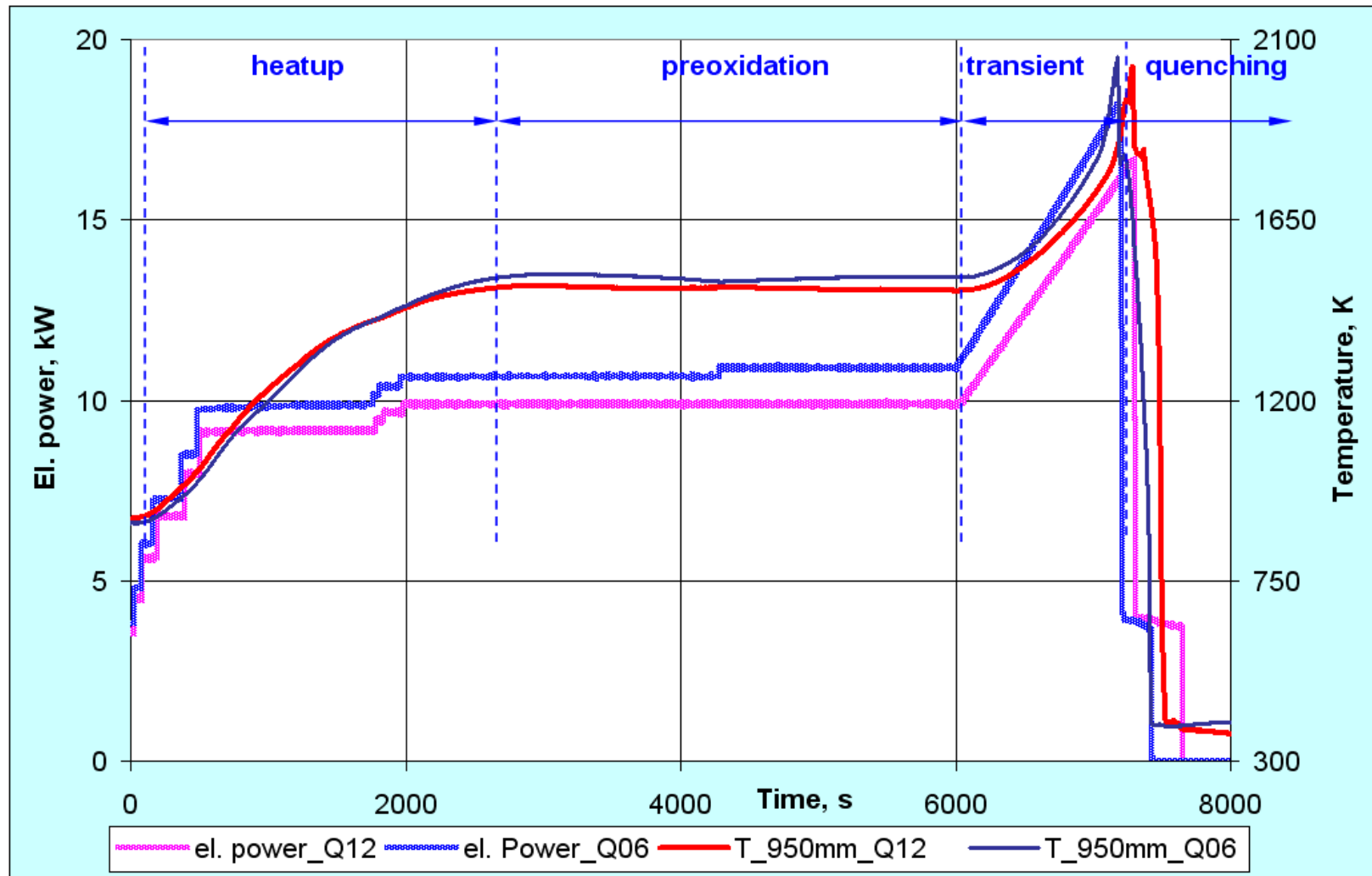
Pretest modelling support:

1. **SCDAP/SIM simulations:** *Paul Scherer Institute, Switzerland.*

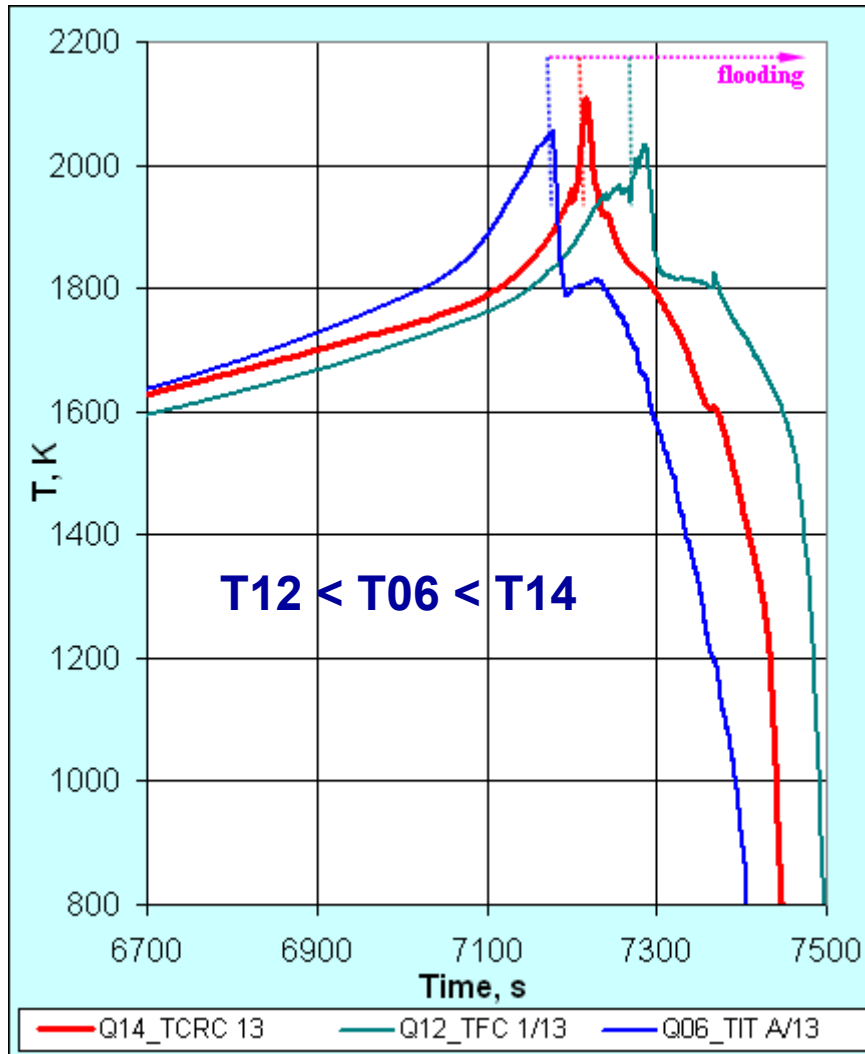
2. **ICARE/CATHARE simulations:** *Kurchatov Institute, Moscow, with support from IRSN Cadarache.*



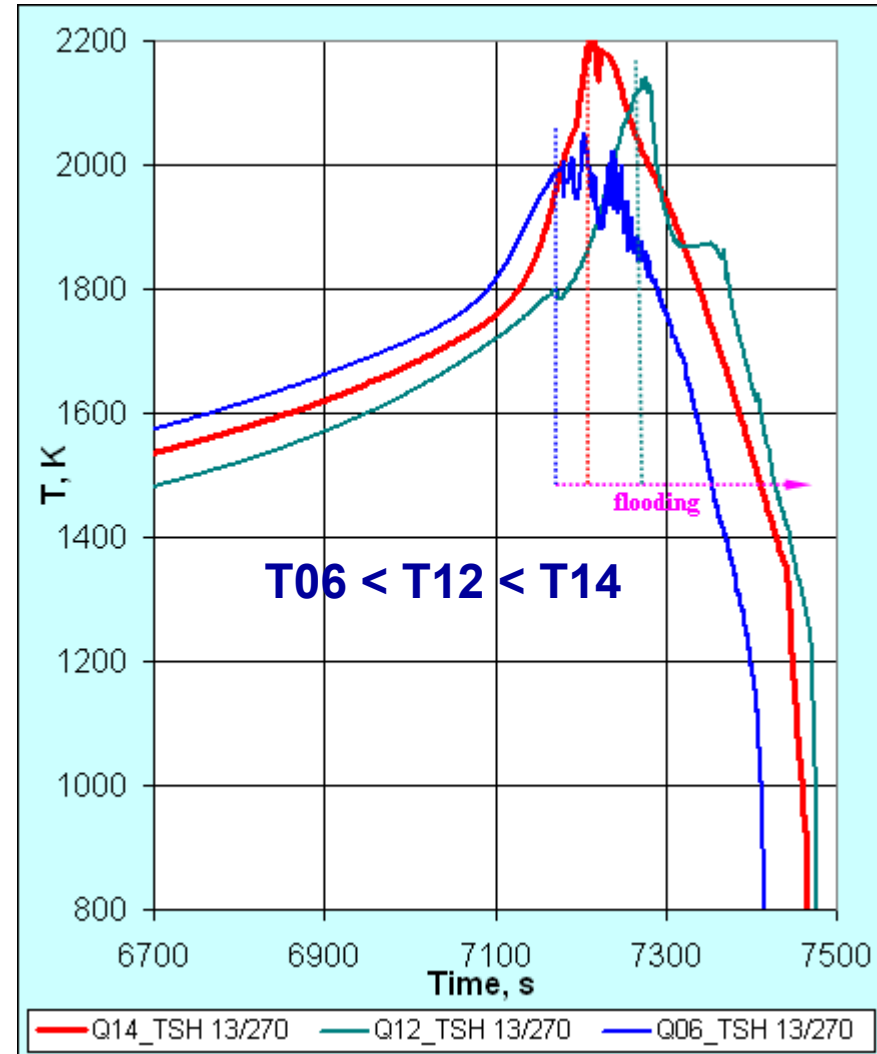
Test performance: el. power profile in accordance to the pre-test calculations provided good reproduction of temperature history in comparison with the reference test QUENCH-06



Comparison of transient and reflow phases for
QUENCH-14 (M5), QUENCH-12 (E110), QUENCH-06 (zry-4):
 similar escalation before reflow



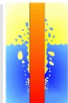
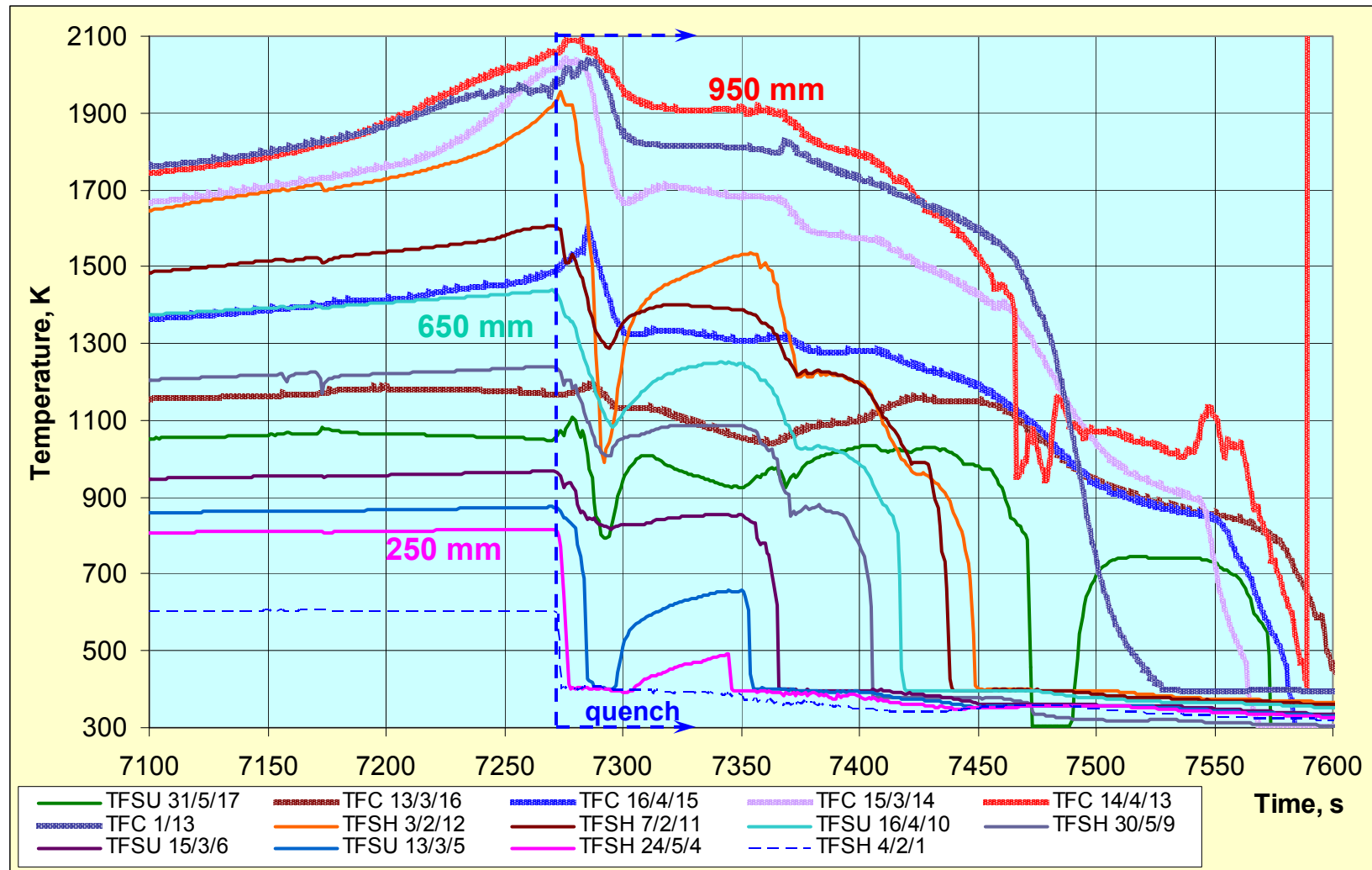
bundle temperature at hot elevation of 950 mm



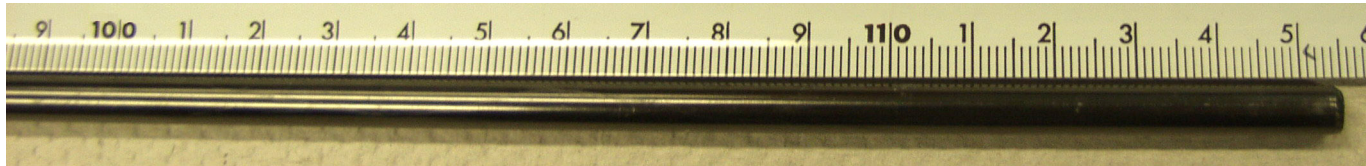
shroud temperature at hot elevation of 950 mm



QUENCH-12, quench phase: selected reading of the bundle thermocouples. Quench front propagation.
 Cooling of the bundle during ~350 s (similar to Q-06 and Q-14)



QUENCH-12: withdrawn Zr1%Nb corner rods



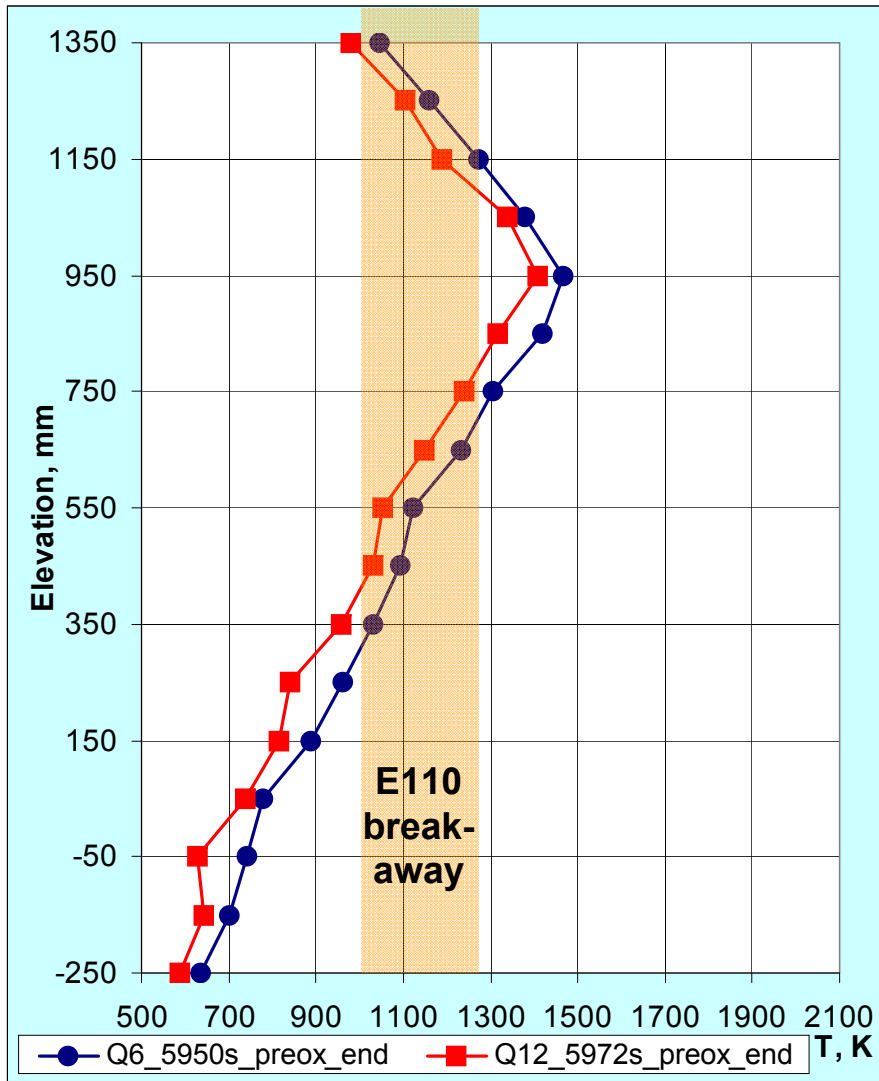
corner rod B after pre-test (800 °C, oxide layer thickness less of 5 µm)



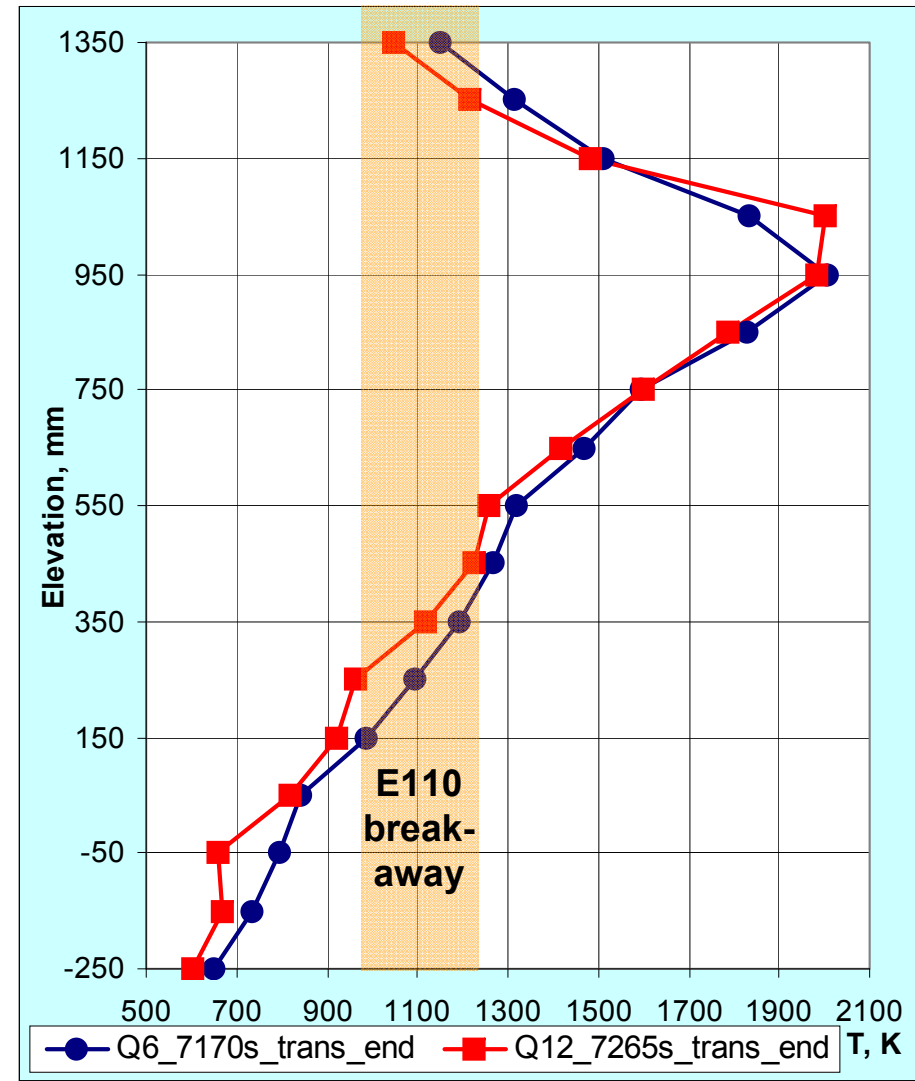
corner rods withdrawn during the test:
spalling of the outer skin of oxide layer due to breakaway oxidation.

D – withdrawn after pre-oxidation,
F – withdrawn before reflood,
B – withdrawn after test.

Axial bundle temperature profiles for QUENCH-06 and QUENCH-12 on beginning and end of transient phase



beginning of transient

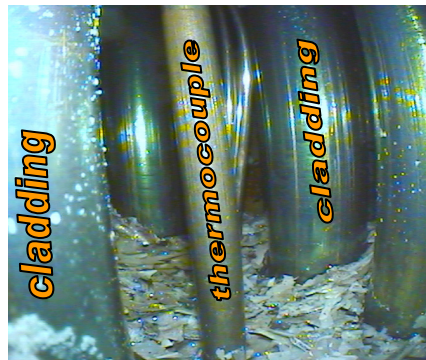


end of transient

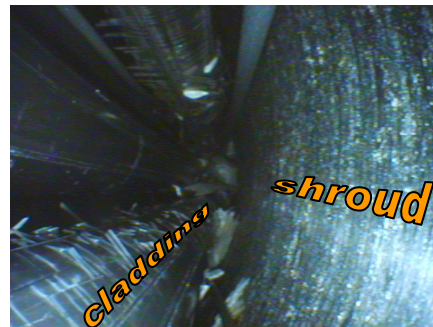


QUENCH-12: post-test videoscope observations of breakaway oxidation at different elevations of the bundle

T_{min}



-400mm:
spalled oxide scales
as debris
at the bundle bottom



400 mm:
circumferential spalling
of the oxide layer
on the surface
of fuel rod simulator cladding



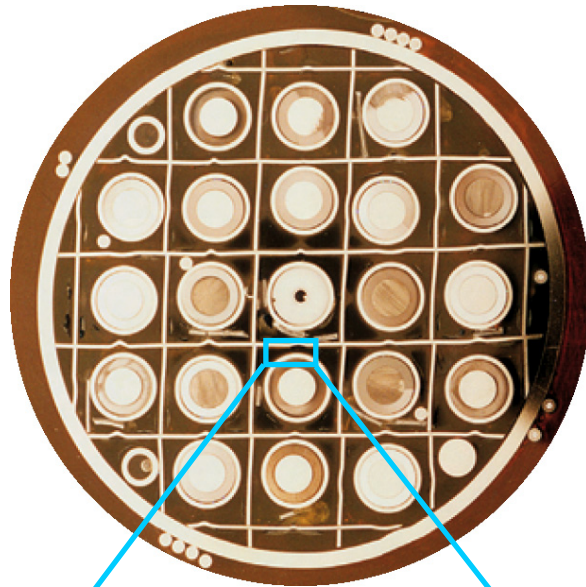
650 mm:
spalled oxide scales
at shroud and cladding



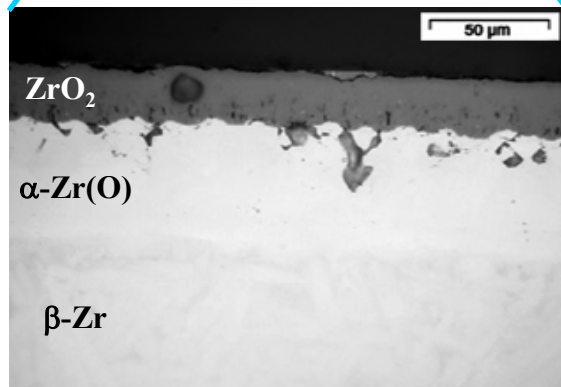
T_{max}

900 mm:
circumferential
and longitudinal cracks
at the cladding;
nodular breakaway
corrosion
at the shroud

Comparison cross-sections of **QUENCH-06** and **QUENCH-12**
at elevation 550 mm with ZrO_2 thickness $\sim 40 \mu m$



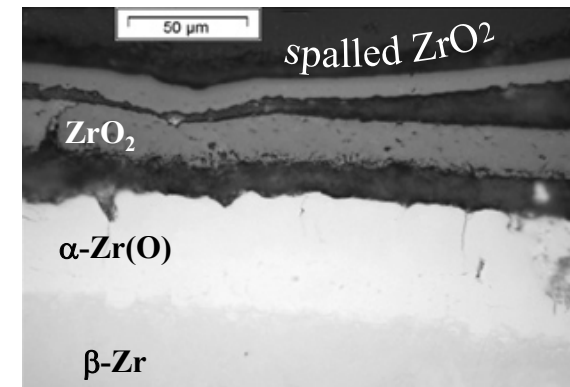
Q06 cross-section



Q06 oxidized cladding

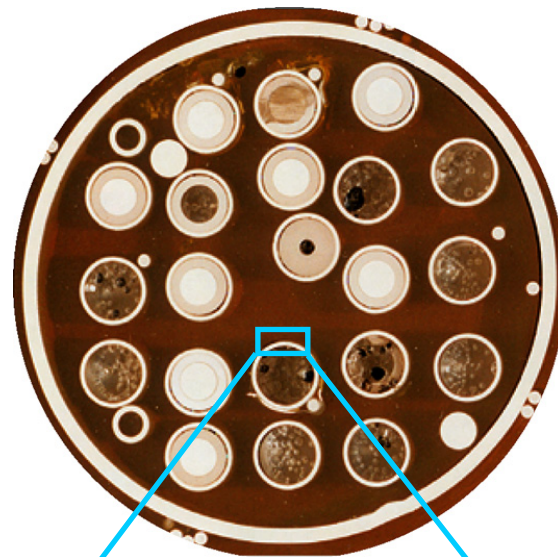


Q12: rubble on spacer grid consists of spalled cladding scales and fragments of partially oxidized cladding

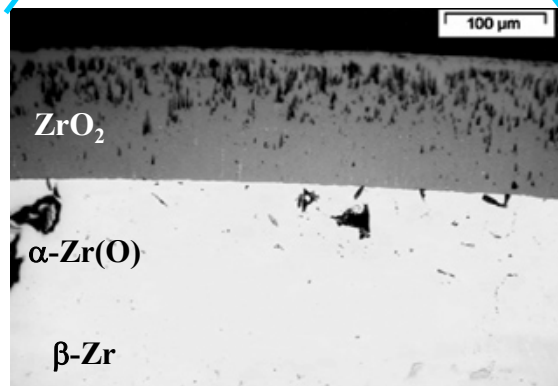


Q12 cladding: spalling of oxide scales due to breakaway effect

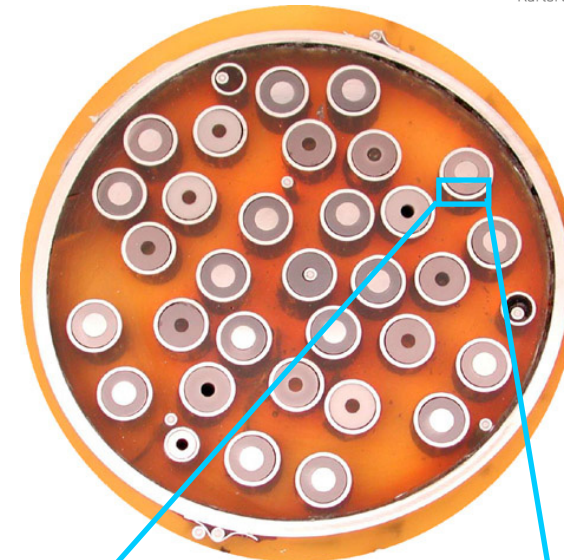
Comparison cross-sections of QUENCH-06 and QUENCH-12 at elevation 750 mm with ZrO_2 thickness $\sim 80 \mu m$



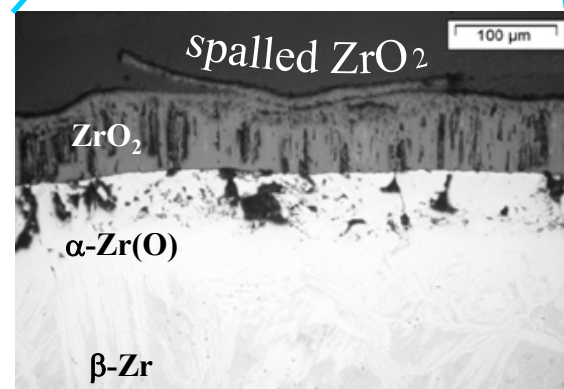
**Q06 cross-section;
few bundle deformation**



Q06 oxidized cladding



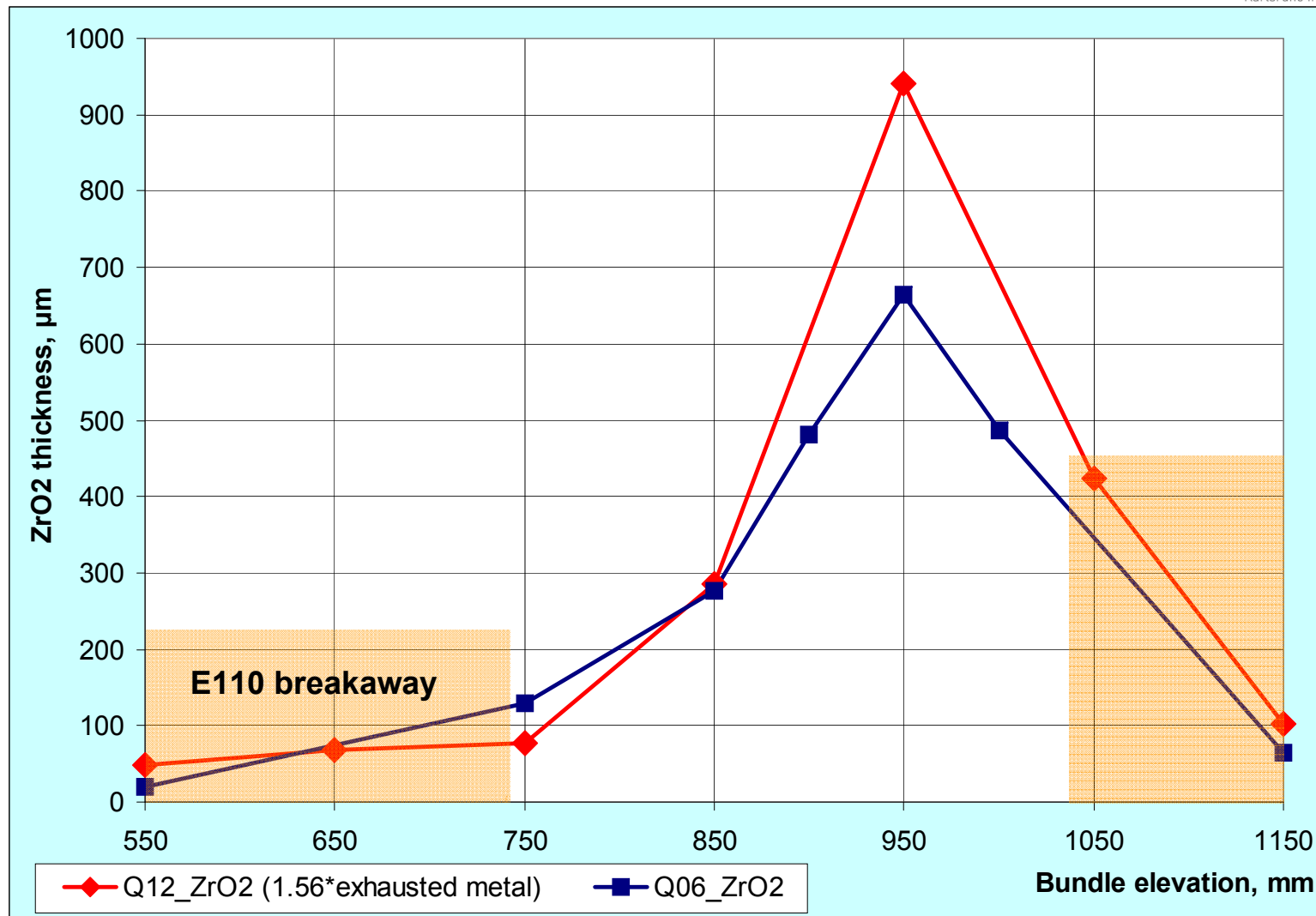
**Q12 cross-section;
moderate bundle deformation**



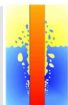
**Q12 cladding: spalling of oxide scales
due to breakaway effect**



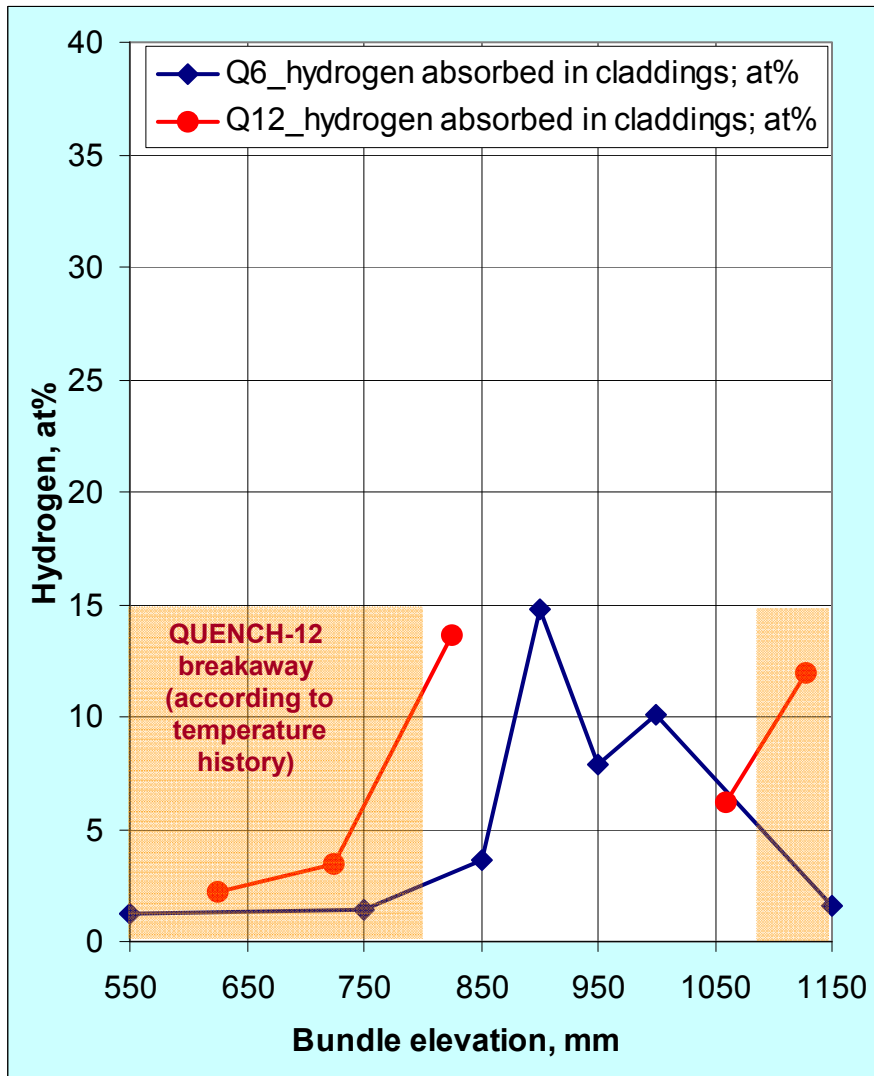
Comparison of averaging oxide cladding thicknesses for QUENCH-06 and QUENCH-12 at all elevations



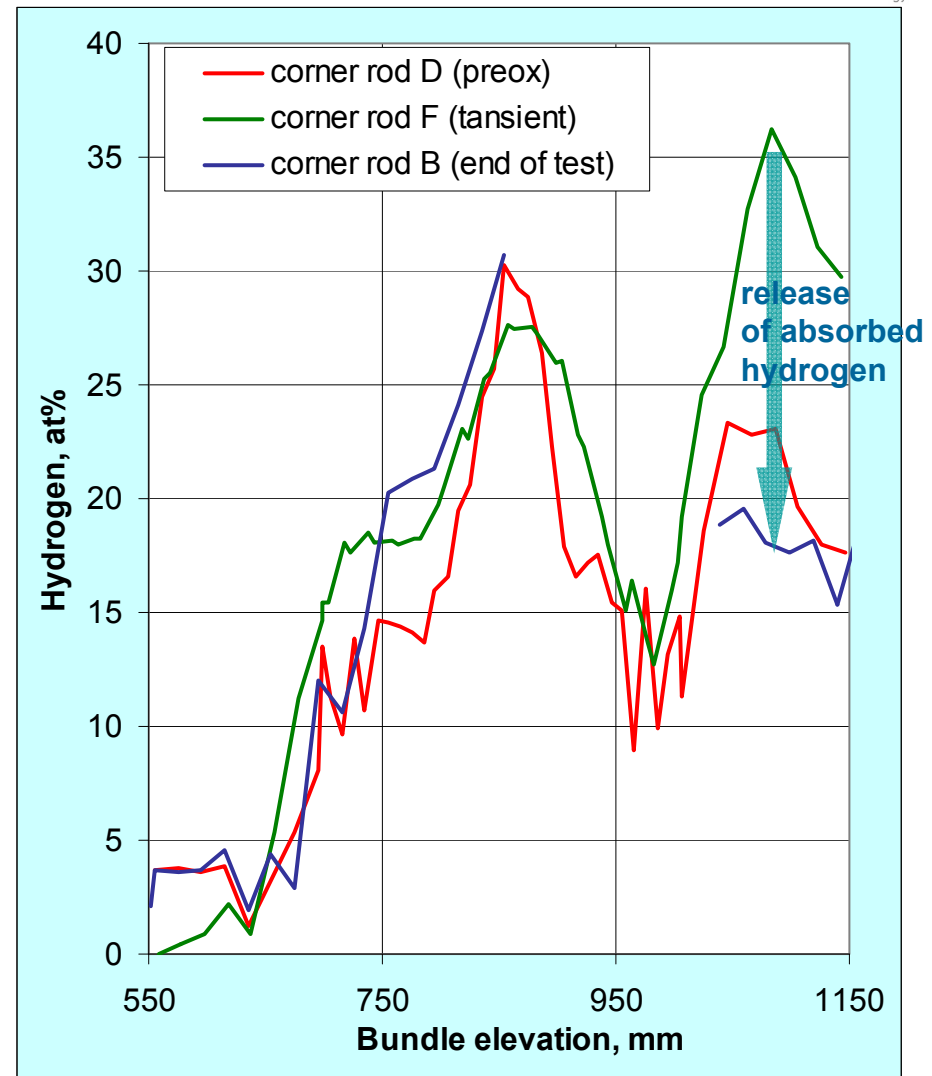
Degree of cladding oxidation is mostly lower for QUENCH-06 (Zry-4) in comparison to QUENCH-12 (E110)



Comparison of hydrogen uptake by bundle during QUENCH-06 and QUENCH-12



Q-06<->Q-12: H₂ uptake in cladding measured by hot extraction



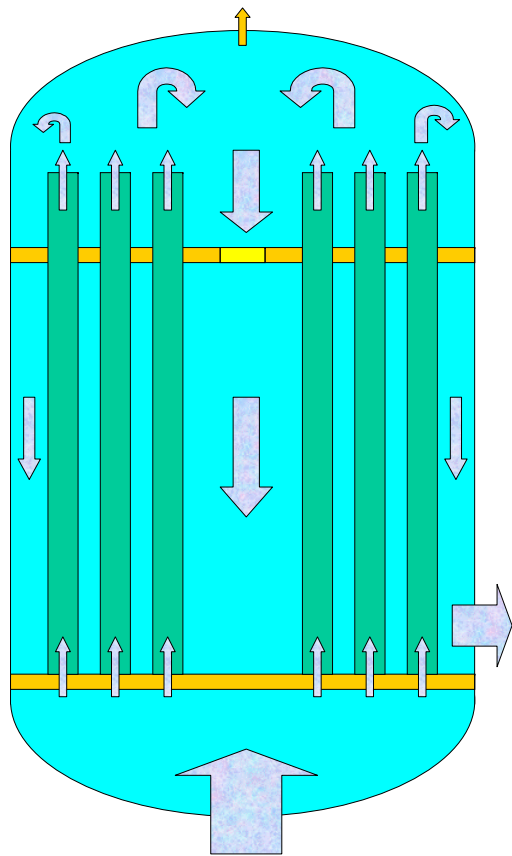
Q-12: H₂ uptake in corner rods measured by neutron radiography



Paks/Ungary cleaning tank incident in April 2003 with destroying of 30 VVER fuel assemblies

Cooling during normal cleaning:

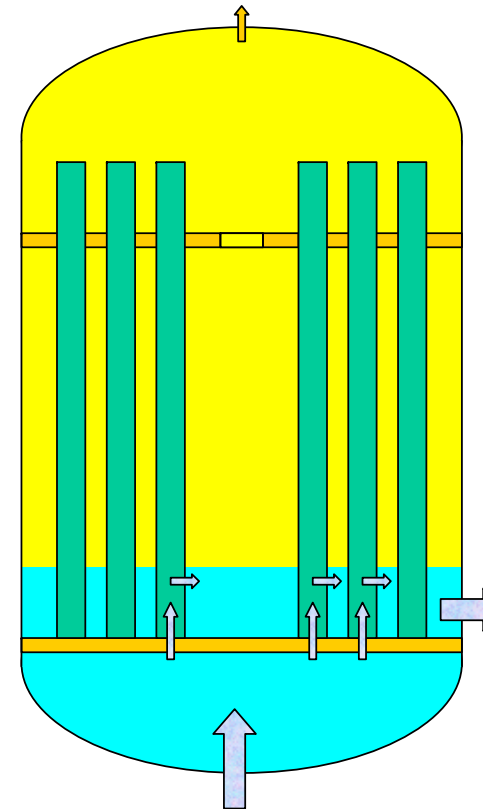
- high flow rate
- closed loop



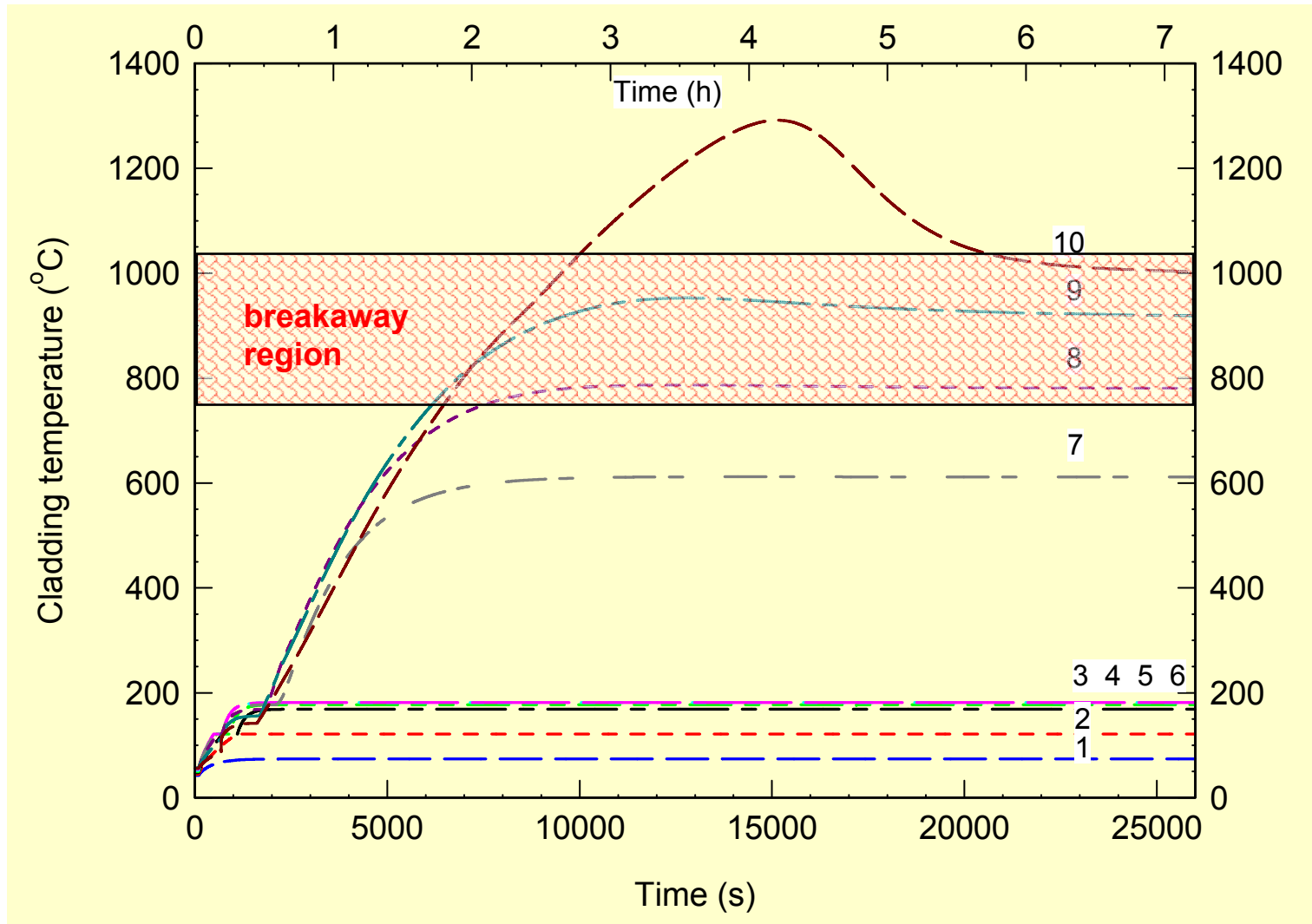
Cooling after cleaning

- low flow rate
- open loop with connection to spent fuel pool
- possibility of by-pass by bundle low head

decay heat for 30 bundle: 241 kW



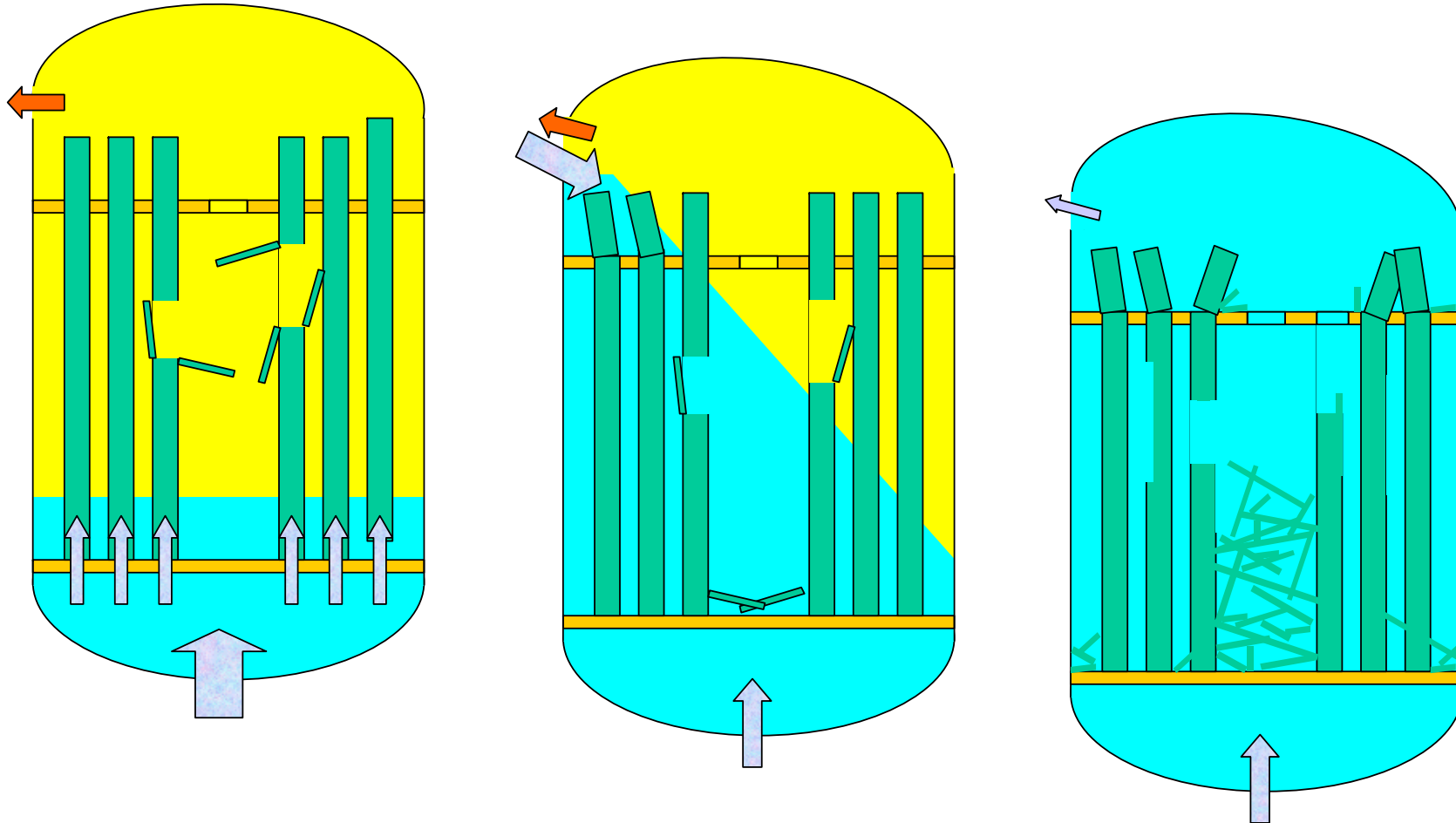
Breakaway long-term oxidation during the Paks cleaning tank incident (destroying of 30 VVER fuel assemblies)



Results of modeling (FRAP-T6 code)



Collapse of VVER-bundles, strong hydrogenated under breakaway conditions



Other important phenomenon: melt formation and oxidation by
QUENCH-06 and QUENCH-12 at elevation 950 mm

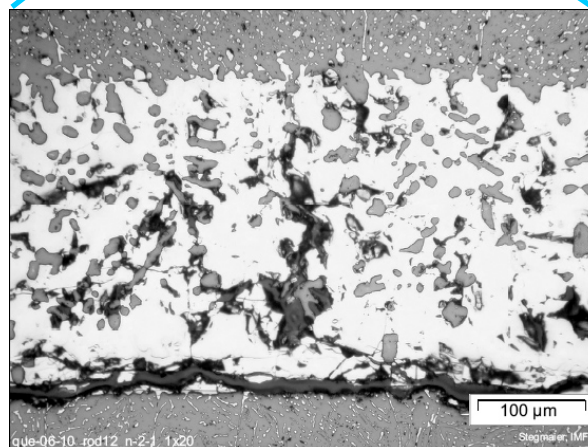
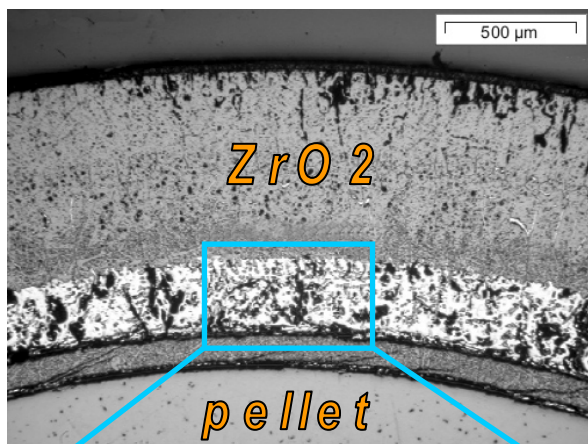


**Q06 - bundle geometry intact->
good coolability;
melt localized between pellet and ZrO₂ layer**

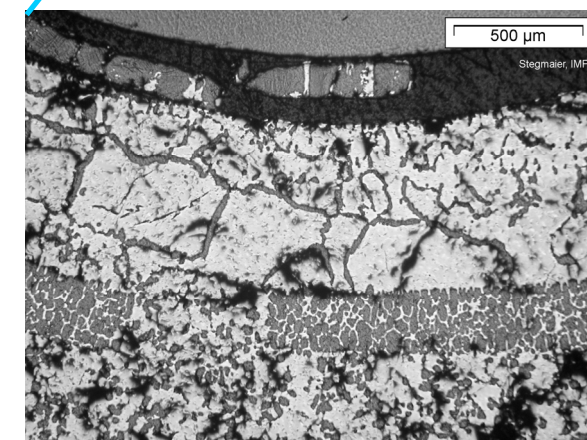
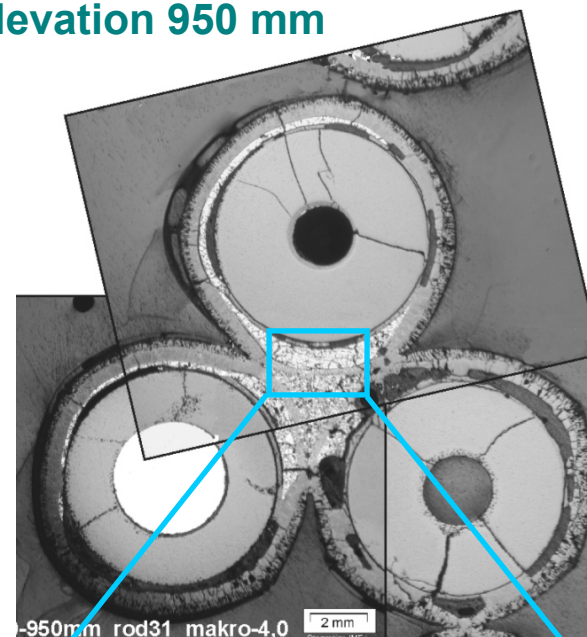


**Q12 - bundle geometry destroyed->
declined coolability;
molten pools formation inside rod clusters**

Melt formation and oxidation by QUENCH-06 and QUENCH-12 at elevation 950 mm

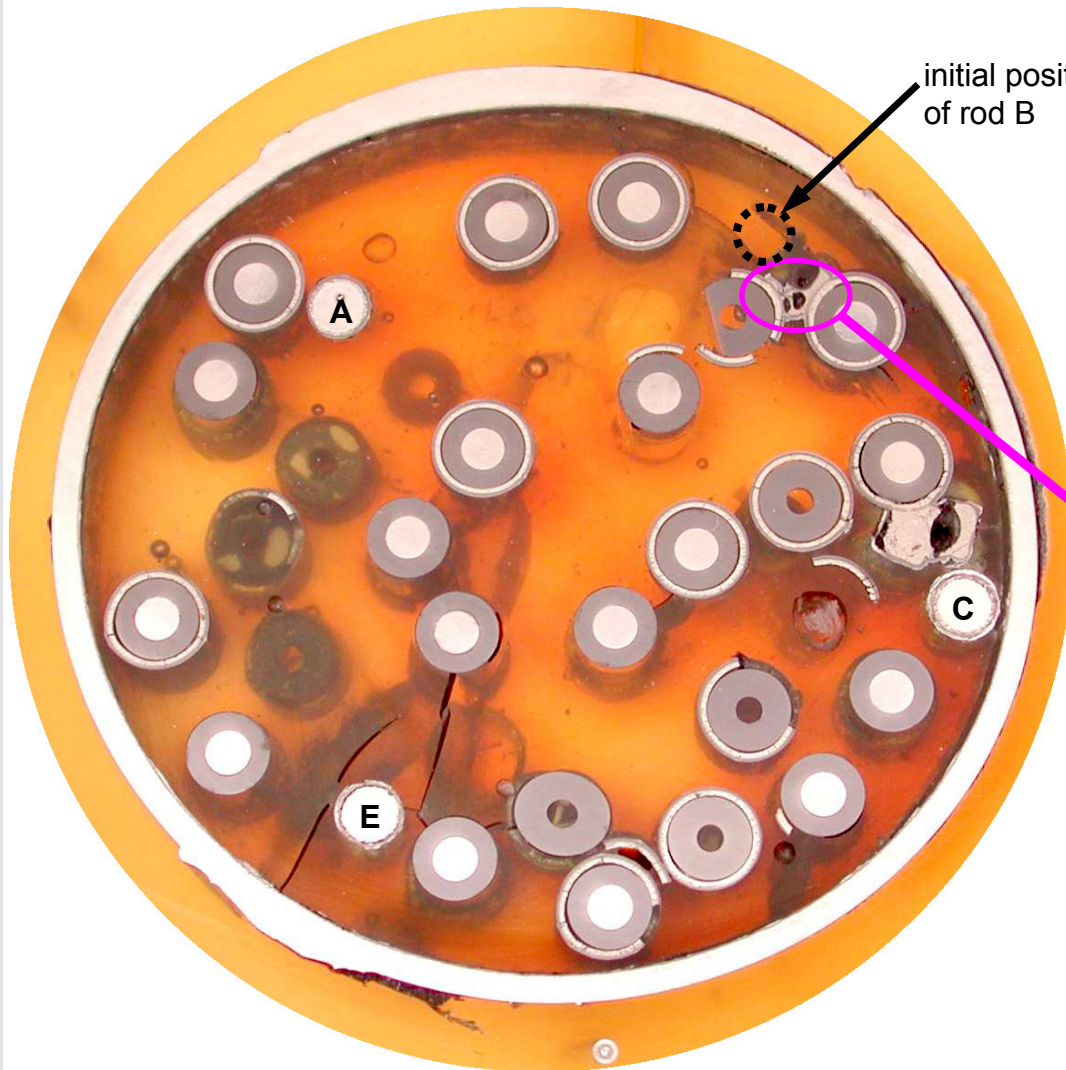


**Q06: melting of cladding metal layer,
precipitates formation on cooldown**

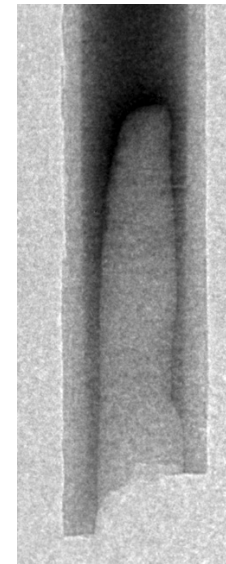


**Q12: molten pool between rods,
precipitates formation due to melt oxidation in steam**

QUENCH-12: melting of corner rod B



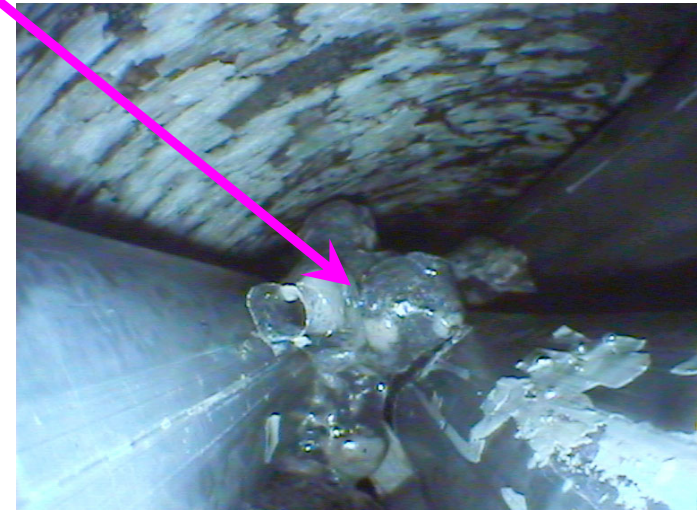
initial position
of rod B



1035 mm

neutronography
shows the deep hole
at the place
of melted out β -Zr

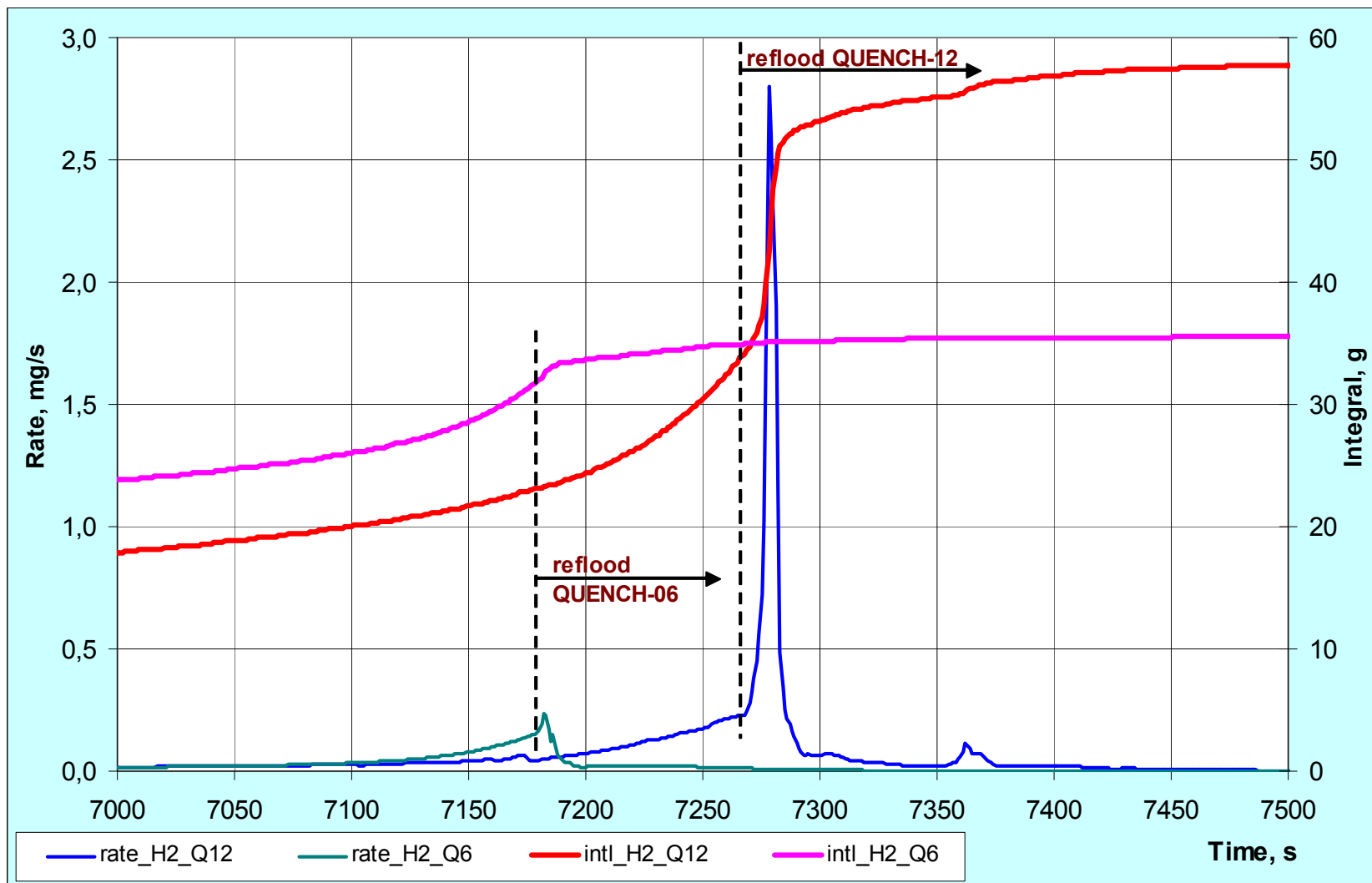
1010 mm



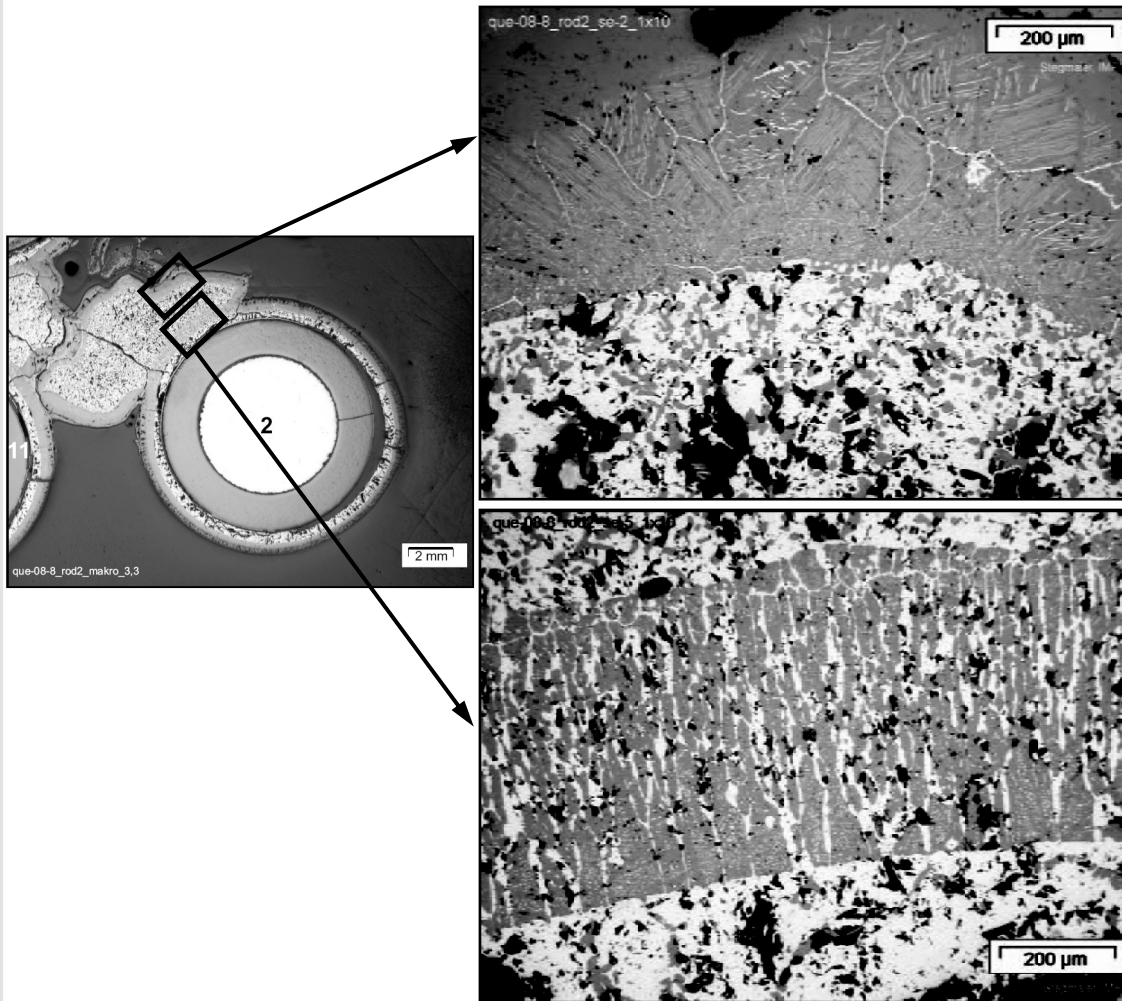
850 - 900 mm: melt formation in bundle at
the position of melted corner rod B



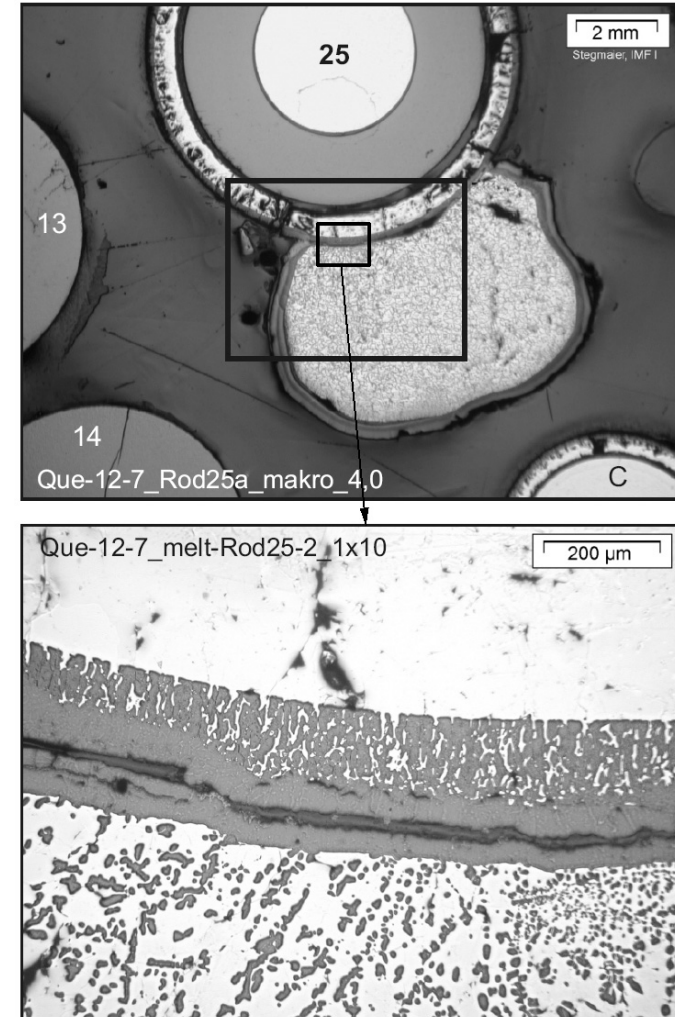
Comparison of hydrogen release during **QUENCH-12** and **QUENCH-06**



Comparison of post-test cladding and melt structures for Q-08 and Q-12



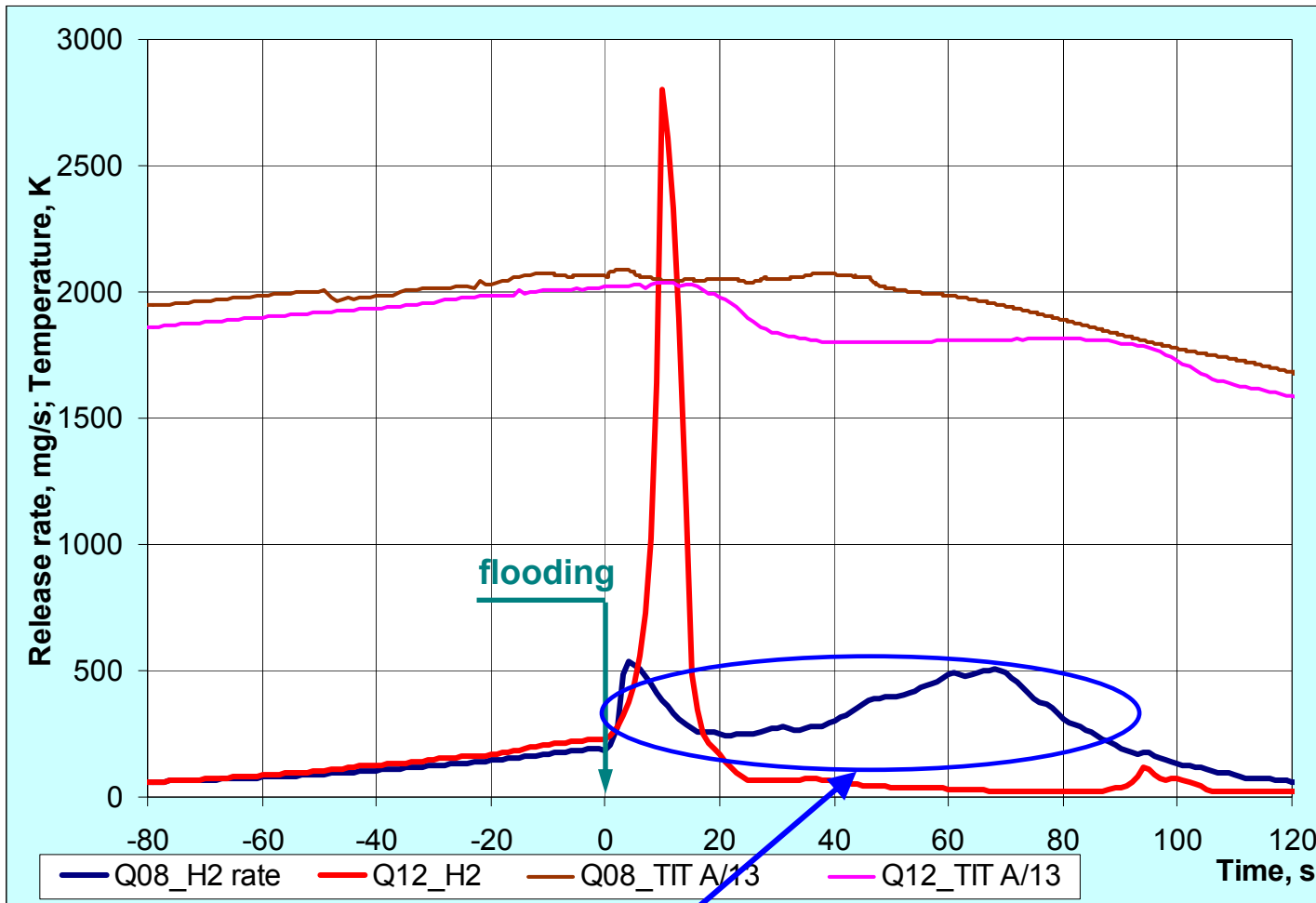
Q-08, 860 mm



Q-12, 850 mm



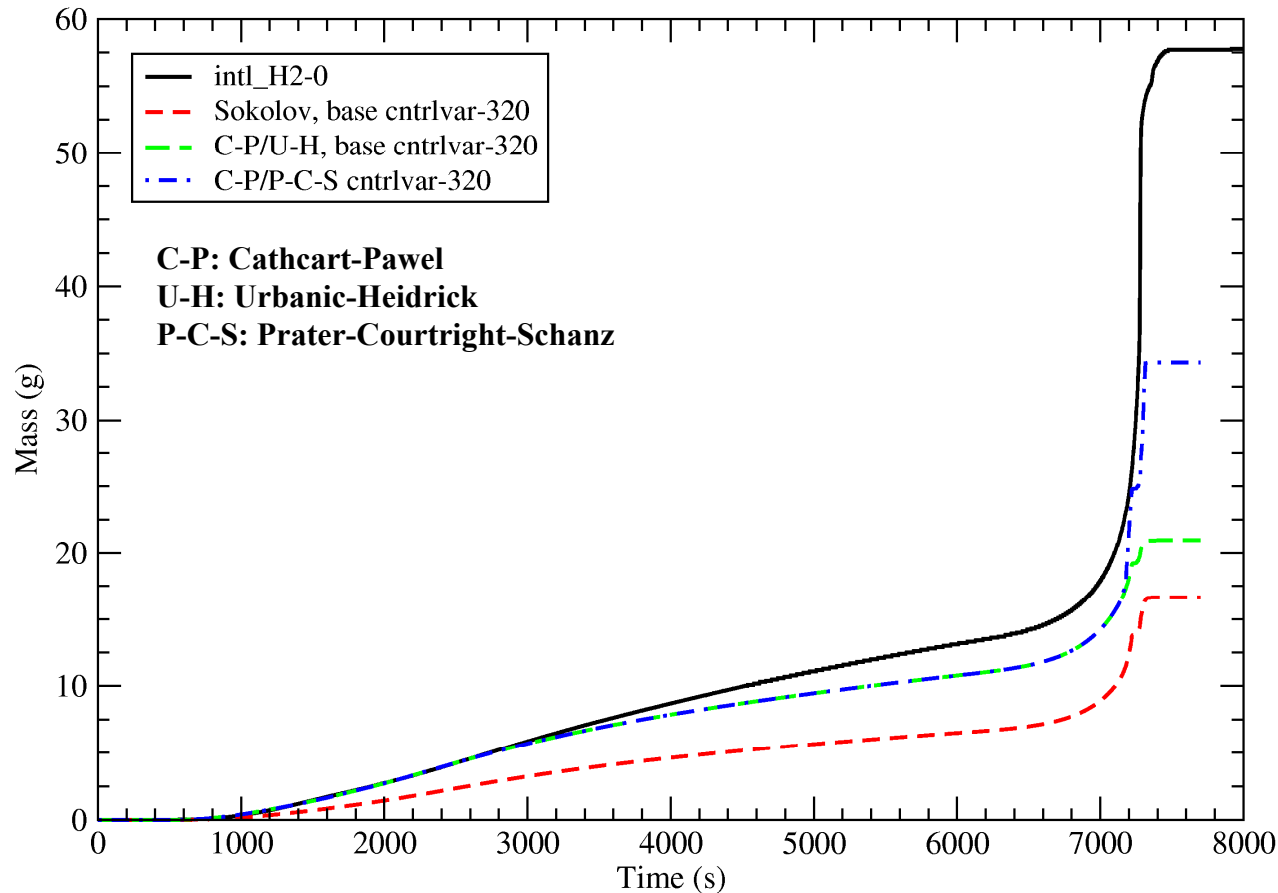
Comparison of hydrogen release during reflood
 for Q-08 test (oxidation before transient 270 μm ; significant melt oxidation)
 and Q-12 test (oxidation before transient 160 μm ; minor melt oxidation)



Long duration of hydrogen production during the quench phase in case of significant melt oxidation (Q-08)



QUENCH-12: calculated and measured hydrogen generation /J. Birchley, PSI/

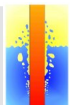


**Despite the similar thermal response through almost the entire sequence,
all of the calculations underestimated the oxidation.**



CONCLUSIONS

- The QUENCH-12 experiment was carried out to investigate the effects of VVER materials and bundle geometry on core reflood, in comparison with the test QUENCH-06 (Zry-4-cladding) with western PWR geometry.
- During the pre-oxidation and transient phases the E110 cladding alloy is susceptible to breakaway oxidation within relative broad temperature range (1050 – 1300 K). Oxide scale of layered type showed spalling into sub-layers and loss of fragments, which were collected at spacer grids and bundle bottom.
- The breakaway oxidation was accompanied by hydriding of claddings and shroud with the result of material embrittlement, which can lead to a severe degradation of the bundle during quenching as was demonstrated in the Paks accident.



CONCLUSIONS (cont.)

- Melting point of claddings and shroud metal layer was reached at the peak temperature elevations of 950 – 1050 mm. Contrary to QUENCH-06, where melt was confined between pellets and the outer cladding oxide layer, the melt in QUENCH-12 has in places dissolved the surrounding oxide layer. As a result, non-coherent melt relocation, melt pool formation, and minor melt oxidation were observed.
- The total hydrogen production was 58 g (QUENCH-06: 36 g), 24 g of which were released during reflood (QUENCH-06: 4 g). Three possible sources of increased hydrogen production during reflood: 1) interaction of steam with new metal surfaces developed by spalling of oxide scales damaged during pre-oxidation phase because breakaway effect; 2) release of hydrogen absorbed in metal by breakaway during pre-oxidation and transient phases; 3) moderate melt oxidation released into space between rods.
- The S/R5 code adequately reproduced the QUENCH-12 thermal transient. Both the Cathcart-Pawel and Sokolov correlations underestimated the oxidation kinetics, but preliminary analysis indicates that the comparison with QUENCH-06 is consistent with the change in the bundle configuration and cladding material; in particular breakaway effect may have enhanced the oxidation.

